



outgassing rate from a garnet ferrite used in an SF<sub>6</sub>-type isolator and found that it is about 34 times larger than that of stainless steel, after a baking process at 80°C. Since the surface area of the ferrite is small enough, this is acceptable for an ultra high vacuum system. Residual gas was analyzed in a high power test described below.

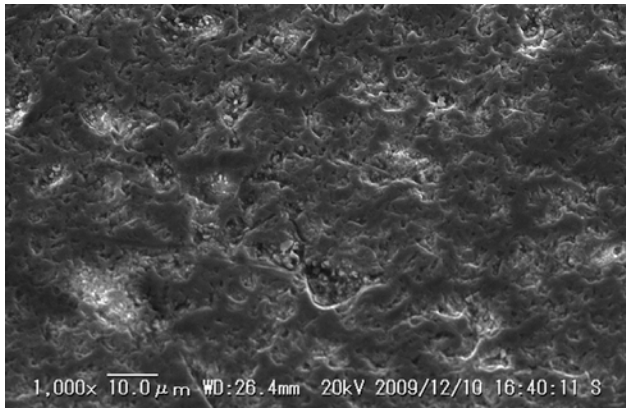


Figure 2: SEM image of a garnet-ferrite surface.

### Bonding of Ferrite on Copper

The development of a bonding method of ferrite pieces on a copper surface was the most time consuming issue in this R&D. Because the difference in the coefficient of the thermal expansion between ferrite and copper is large, the usual brazing method with silver solder could not be applied. The successful bonding method was soldering with a copper ring around segmented ferrite pieces. It simultaneously satisfied mechanical strength and thermal conductivity. The thermal conductivity was 9.3 times larger than that of an electrically conducting adhesive (AMICON<sup>®</sup>). A ferrite located in an isolator is shown in Fig. 3.



Figure 3: Ferrite located in a prototype isolator.

## HIGH POWER TEST

### Experimental Setup

Figure 4 shows a prototype isolator and a setup for a high power test. The waveguide section including the isolator was evacuated by a sputter ion pump with a pumping speed of 45 L/s for N<sub>2</sub>. The transmitted and

reflected RF powers were measured using directional couplers located upstream/downstream of the isolator.

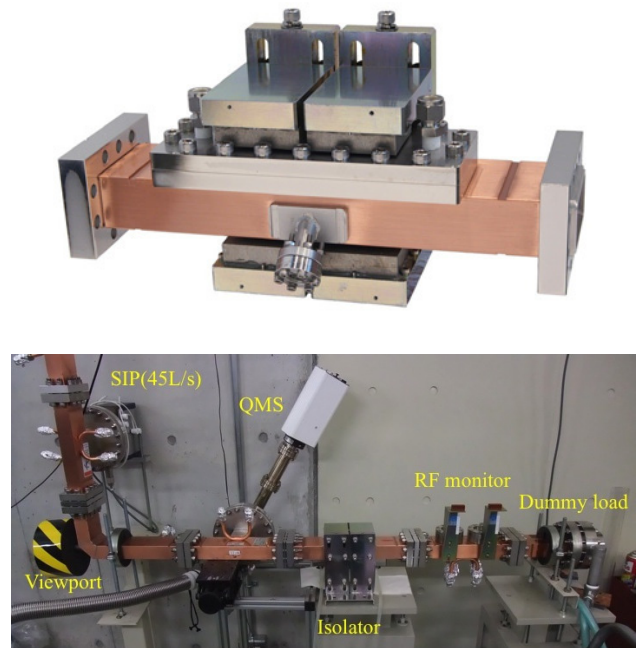


Figure 4: Prototype vacuum isolator (above: a viewport is located to observe ferrite surface) and setup for a high power test (below).

The temperature of the ferrite surface was measured through a BaF<sub>2</sub> window by a radiation thermometer. The outgas components were measured by a quadrupole mass spectrometer (QMS). A CCD camera was also installed at a viewport to observe the discharge lights.

### RF Conditioning

An RF conditioning was performed with a pulse width of 2.5 μs and a repetition rate of 10 pps. An example of the RF conditioning in a normal (forward) direction is shown in Fig. 5.

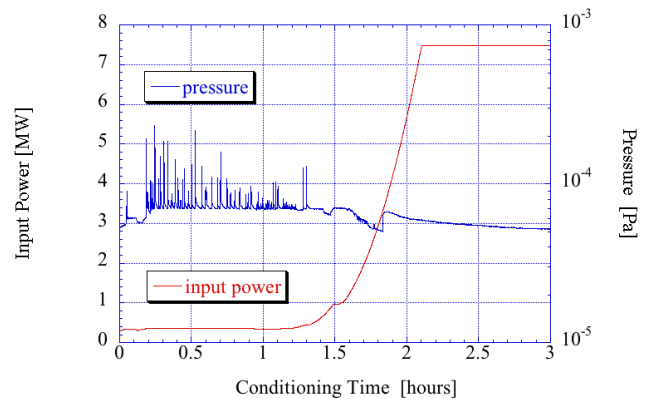


Figure 5: Input power and vacuum pressure history of RF conditioning of prototype isolator (normal direction).

Spike-like pressure risings were observed below 1 MW and they decreased around 4 MW. No discharge light was observed during the conditioning. Such a pressure rising

history resembles ceramic RF windows or SiC dummy loads. Finally, the input power reached up to 45 MW.

*RF Characteristics*

The RF parameters were measured in a high power test. The insertion loss measured in a forward direction of the isolator maintained 0.3 dB to a maximum input power of 45 MW. This suggests that a circulator using this ferrite will work at this power level. Next, the direction of the RF input was reversed to measure the isolation. The isolation worsened as the input power was increased (Fig. 6). The isolation measured in a low power measurement was 16 dB and became 9 dB at an input power of 30 kW. The resonance frequency in a ferrite apparently varies as a function of the input power, and this frequency shift must be investigated.

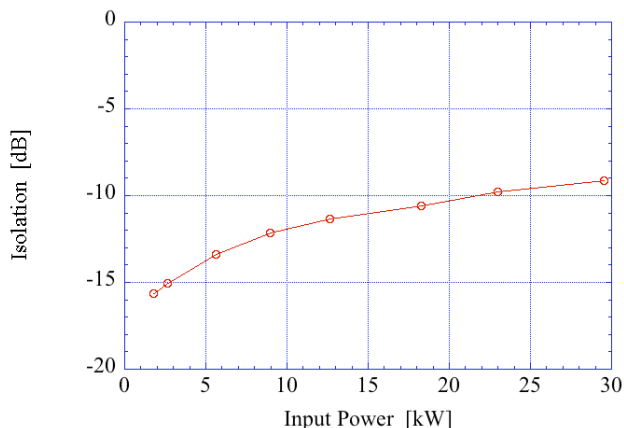


Figure 6: Isolation of prototype isolator as a function of input power.

To improve the isolation in a frequency region below 100 kW, the lengths of the ferrite pieces and the external magnets were expanded in a production version of the isolator. This improved the isolation to 32 dB in a low power measurement (Fig. 7).

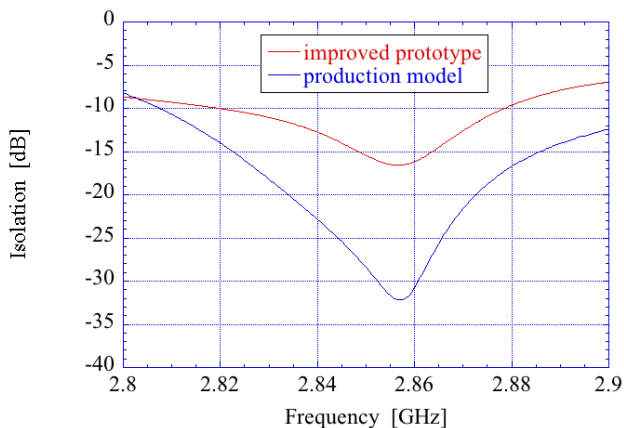


Figure 7: Improvement of isolation by expanding ferrite and external magnets.

Although a high power test for the production model is under going, the isolation of larger than 20 dB was confirmed in a power range below 20 kW.

*Vacuum Characteristics*

The pressure in the waveguide system without the isolator reached  $3 \times 10^{-6}$  Pa after 17 hours of pumping; it was  $2 \times 10^{-5}$  Pa with the isolator. This difference reflects the outgassing from the ferrite in the isolator. Based on a residual gas analysis by the QMS,  $H_2$  and  $H_2O$  were dominant (Fig. 8).

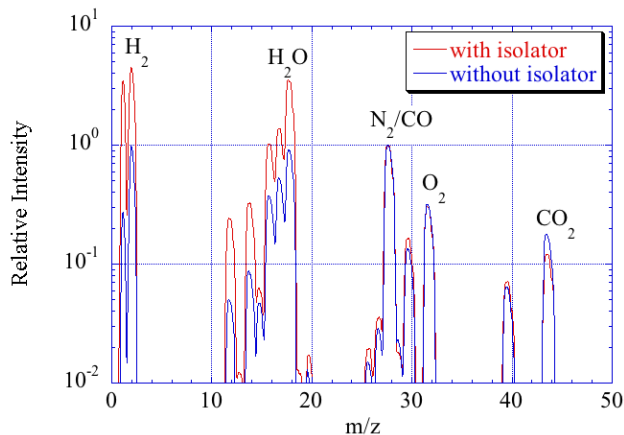


Figure 8: Residual gas spectrum with/without isolator (relative intensity was normalized for  $N_2/CO$ ).

The water vapor was probably absorbed in the ferrite during the tuning in the factory for a week. Therefore, the isolator was baked out with hot water at 80°C. The achieved pressure was improved to  $1 \times 10^{-5}$  Pa and was further improved to  $3 \times 10^{-6}$  Pa in a production model of the isolator.

**SUMMARY**

To upgrade the  $SF_6$  waveguide system of the injector section of the SPring-8 linac, we developed a vacuum-type isolator. The RF and vacuum characteristics satisfied the required speculations. A vacuum-type circulator that works up to 10 MW, is also being developed and its high power test is scheduled this year. The  $SF_6$  waveguide system for the injector section will be replaced with vacuum waveguides next year.

**REFERENCES**

[1] H. Hanaki et al., “Enhancements of Machine Reliability and Beam Quality in SPring-8 Linac for Top-Up Injection into Two Storage Rings”, PAC’05, Knoxville, May 2005, p. 3585 (2005); <http://www.JACoW.org>.  
 [2] S. Suzuki et al., “Initial Data of Linac Preinjector for SPring-8”, PAC’93, Washington D.C., May 1993, p. 602 (1993); <http://www.JACoW.org>.